PRAMANA
— journal of
physics

Vol. 83, No. 5
November 2014
pp. 749–759

Role of near threshold resonances in intermediate energy nuclear physics

B K JAIN[1,*] and N J UPADHYAY[2]

[1]UM-DAE Centre for Excellence in Basic Sciences, Mumbai University, Mumbai 400 098, India
[2]Department of Physics and Astronomy, Louisiana State University, Baton Rouge, LA 70803, USA
*Corresponding author. E-mail: brajeshk@gmail.com

DOI: 10.1007/s12043-014-0868-5; ***e*Publication:** 4 November 2014

Abstract. The presence of a resonance close to the threshold strongly effects the dynamics of the interacting particles at low energies. Production of ^{12}C, the element for life, in ^{4}He burning in Sun is a classic example of such a situation. In intermediate energy nuclear physics, this situation arises in the interactions of an η-meson with a nucleon and that of a K^--meson with a proton at low energies, where both these systems have a resonance or a bound state near their thresholds, resulting in a strong attractive interaction. If putting these mesons in nuclear environment produces a strong attraction, it is possible that, in nature there may exist η- and K^--nuclear bound states. Such a tantalizing possibility has led to experimental and theoretical programmes to search for them. These efforts have produced positive results. This paper gives a brief critical overview of these studies, emphasizing especially the efforts led by Bhabha Atomic Research Centre (BARC).

Keywords. η-mesic nuclei; kaon bound states; binding energies.

PACS Nos 13.75.Jz; 21.85.+d; 25.80.Nv; 13.75.−n

1. Introduction

Proximity of a resonance to the threshold of two interacting particles strongly influences their dynamics at low energies. The classic example of this is the crucial role played by the ^{8}Be resonance and the famous Hoyle state (the 0^+, ^{12}C* 7.65 MeV resonance), (which are close to the α-α and α-^{8}Be thresholds, respectively) in producing ^{12}C, the element for life, in ^{4}He burning in Sun. In intermediate energy nuclear physics, the $S_{11}(1535)$ resonance and the $\Lambda(1405)$ bound state, which are close, respectively to the ηN and the $K^- p$ thresholds (figure 1) play important roles in making the interaction between these pair of particles strongly attractive at low energies. The possible consequence of this is the likelihood of the existence of η-nucleus and K^--nucleus bound states.

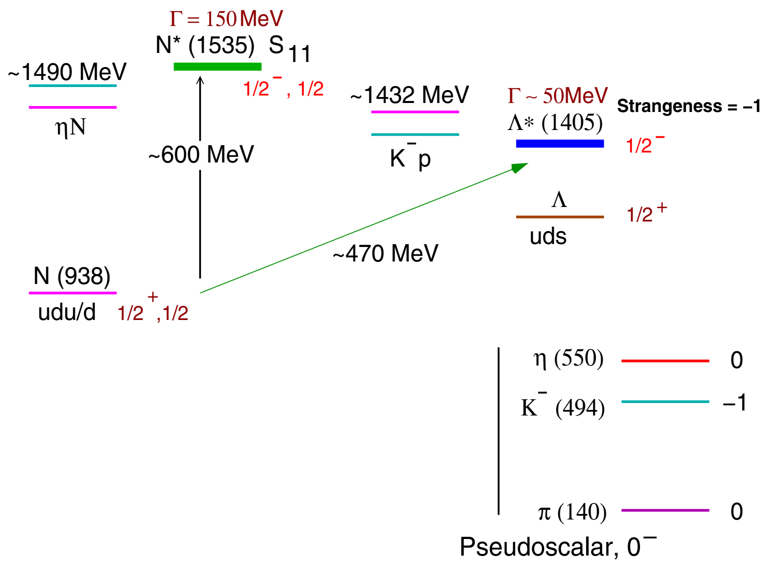

Figure 1. Relevant mesons and baryonic resonances.

To explore this tantalizing possibility, several experimental and theoretical efforts have been made. They have yielded positive results, though not very conclusive (for review, see [1,2]). We present in this paper a brief critical review of these studies.

2. η-nucleus system

2.1 *Experimental*

The first indication of the strong attractive η-nucleus interaction came from the experimental observations on the $pd \to {}^3\mathrm{He}\,\eta$ reaction from 0.2 to 11 MeV above the threshold at Saturne Laboratory, Saclay. A surprising observation of these measurements was the sharp rise in the production amplitude of this reaction as the energy approached the threshold from higher energies. This was seen as an indication of the strong attractive η-^{3}He interaction and its relation to the formation of a quasibound state in ^{3}He.

Observation of an actual η-nucleus quasibound state was made recently using photon beam at Mainz Microtron Facility (MAMI) and the proton beam at the COSY Facility, Jülich. Both these experiments follow the strategy that,

(1) The dynamics of the η-meson is governed by the S_{11}, $J^\pi(\text{spin}^{\text{parity}}) = \frac{1}{2}^-$ resonance, the excited state, $N^*(1535)$ of the nucleon. This state is just 49 MeV above the ηN threshold and has a width $\Gamma = 150$ MeV. It, thus, covers the whole low-energy region of the ηN interaction. It decays into πN and ηN channels with about equal probability.

(2) For an η bound state the S_{11} resonance cannot decay into ηN in free state. It can decay only to πN. Furthermore, as the Fermi momentum is not large, S_{11} is practically at rest in the nucleus. Consequently, the πN emerge out back to back.

Thus, both the experiments detect a pion and a nucleon in coincidence with their 4-momenta fully measured.

2.1.1 *Photoproduction.* The experiment on photoproduction of η on ^{3}He, $\gamma\,^3\mathrm{He} \rightarrow \pi^0\,p\,X$, is done by the TAPS Collaboration [3] using MAMI, where the η-meson was claimed to form a quasibound resonance with a nucleus as light as ^{3}He. The inclusive cross-sections for the $\gamma\,^3\mathrm{He} \rightarrow \eta\,X$ reaction was measured with the beam energy ranging from the threshold to 820 MeV and a resonance structure was found above the η production threshold in the coherent $\gamma\,^3\mathrm{He} \rightarrow \eta\,^3\mathrm{He}$ cross-sections, while a peak was seen slightly below the threshold in the $\pi^0 p$ decay channel. The mass and width of the resonance extracted from these cross-sections were reported to be $[(-4.4 \pm 4.2) - i\,(25.6 \pm 6.1)]$ MeV.

2.1.2 *Proton-induced production.* The production of proton-induced η-mesic nucleus has recently been carried out by the COSY-GEM Collaboration with a heavy target ^{27}Al [4]. The study of the $p\,^{27}\mathrm{Al} \rightarrow\, ^3\mathrm{He}\,\pi^-\,p\,X$ reaction was done at recoil-free kinematics. Forward going ^{3}He nuclei were measured in coincidence with the $\pi^- p$ pair emerging with the relative angle 180° [4]. Such a set-up is based on the idea of excitation of the $N^*(1535)$ resonance in the medium, which would be produced at rest (apart from Fermi motion) and would eventually decay to $\pi^- p$. The study in [4,5] leads to a discovery of peak structure which has been attributed to an η-^{25}Mg bound state with (13.13±1.64) MeV binding energy (figure 2) and ~5 MeV width.

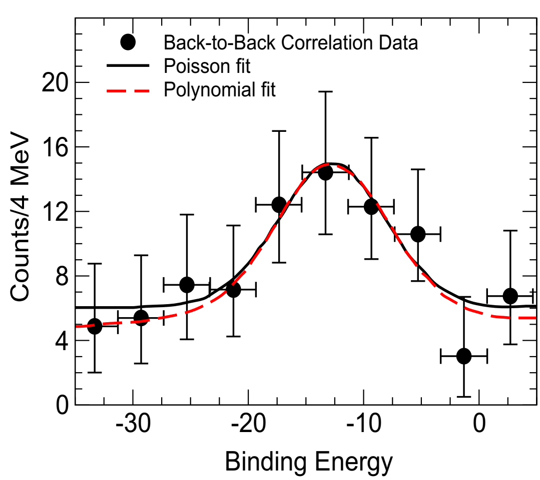

Figure 2. Resonance structure observed in COSY $p\,^{27}\mathrm{Al} \rightarrow\, ^3\mathrm{He}\,\pi^-\,p\,X$. The plot is taken from [4].

The above experiment has been analysed using the optical potential approach within the finite range approximation (FRA) [6]. The authors suggest that the observed peak structure in this experiment, in fact, has coherent contributions from two processes: (i) where an η binds to ^{25}Mg to form an intermediate $^{25}\mathrm{Mg}_{\eta}$ state or (ii) it simply scatters from ^{25}Mg without forming a quasibound state and emerges as a pion through $\eta p \to \pi^0 p$. They found that this quantum interference results in weaker binding (-8 to -10) MeV compared to the experimental value of $\sim$13 MeV.

At COSY the experiment was also performed on the $p\,^6\mathrm{Li} \to {}^7\mathrm{Be}\,\eta$ reaction [7]. The results showed that the cross-sections of this reaction were an order of magnitude lower than those obtained in the case of $pd \to {}^3\mathrm{He}\,\eta$, showing that the cross-sections of the proton-induced η production decrease as a function of the mass number of the target.

A detailed theoretical study of the $p\,^6\mathrm{Li} \to {}^7\mathrm{Be}\,\eta$ reaction with some important observations has also been reported in [8]. Further new experiments are being planned at the COSY laboratory to find more signatures of η-mesic nuclei (see [9] for an overview).

2.2 *Theoretical*

The theoretical works focus on the calculation of the η-nucleus elastic scattering amplitudes and the solutions with η-nucleus potentials using different approaches. The search for ^{3}He-η quasibound states have been reported in the study of the elastic η-^{3}He scattering amplitude using the Wigner's time delay method. For the heavier ^{25}Mg nucleus, calculations have been done using the optical potential approach.

2.2.1 *Time delay method.*

Apparently, this method means that in a scattering process $ab \to ab$, if there is a resonance, the scattering process will take longer time compared to the situation of no resonance. Equivalently, this means that the scattering phase shift δ will show a large variation with energy if measured across a resonance. This fact has been used successfully in the previous works for the analysis of hadron resonances [10]. Application of this method to the analysis of the η-^{3}He elastic scattering is, however, beset with the basic problem of the non-availability of the η-^{3}He elastic scattering data as η beams do not exist. We circumvented this problem by analysing the η-^{3}He reaction, where the elastic scattering information exists in the final-state interaction (FSI), and high precision data exist near the threshold. We analysed these data. The η production was described by a two-step process, where the beam proton interacts with the proton (or neutron) in the deuteron in the first step. This produces a deuteron and a π^+ (or π^0). The pion in the second step interacts with another nucleon in the target deuteron and produces an η. The FSI between η and ^{3}He was incorporated by solving few-body Faddeev-type equations using the finite-range approximation. These studies reproduced the available η production data in p–d fusion near the threshold for η-^{3}He exit channel (figure 3) very well [11]. The η-^{3}He t-matrix in these calculations was introduced in the description of the η-^{3}He scattering wave function ψ^- in the final state,

$$\langle \psi^- | = \langle \vec{k} | + \int \frac{\mathrm{d}\vec{q}}{(2\pi)^3} \frac{\langle \vec{k} \,|\, T_{\eta\mathrm{He}}(\vec{q}) \,|\, \vec{q} \rangle}{E(k) - E(q) + i\epsilon} \langle \vec{q} \,|. \tag{1}$$

Having determined the η-^{3}He t-matrix which fit the $pd \to \eta\,^3$He data well, we applied Wigner's time delay [13] method to it. For our purpose a modification of Wigner's method

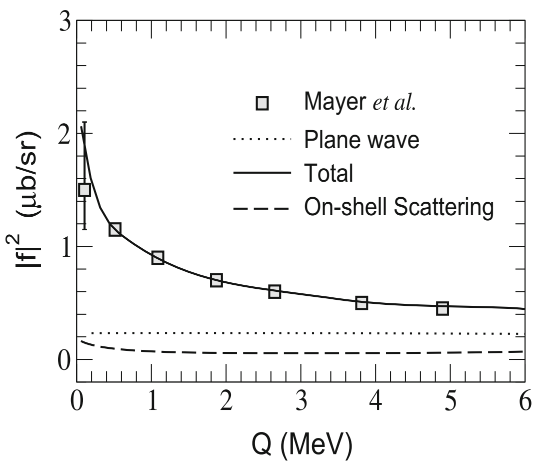

Figure 3. The squared amplitude generated using few-body equations for η-^{3}He FSI with the input of ηN t-matrix corresponding to $a_{\eta N} = (0.88+i0.41)$ fm. Q is the excitation energy given as $Q = E - M_{\rm He} - M_\eta$ with E, $M_{\rm He}$, M_η being the total energy of the η-^{3}He system, mass of ^{3}He and the mass of η-meson, respectively. Figure also shows data from [12].

was done by Kelkar in [14] and an η-mesic state in the η-^{3}He system in agreement with the experiments [14,15] was obtained. Figure 4 shows the time delay results for the elastic η-^{3}He scattering evaluated to locate the η-mesic state.

2.2.2 *Optical potential approach.* The data on ^{27}Al $(p, {}^3\text{He})$ $p\pi^-X$ cross-section from COSY-GEM were analysed in [6]. They considered that the observed peak structure in the experiment arises from the coherent superposition of two reaction processes. In one process, the produced η forms a bound state with ^{25}Mg, and in the other process the produced η comes out of the nucleus via a $\eta p \to \pi^0 p$ reaction. The η-^{25}Mg system was

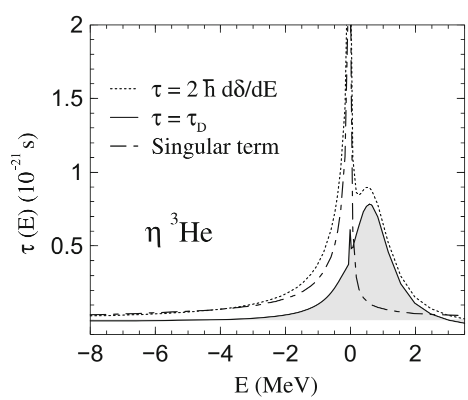

Figure 4. Time delay in elastic η-^{3}He scattering. The plot is taken from [1].

described using a complex optical potential, which was constructed essentially in the '$t\rho$' approximation, where t is the ηN t-matrix. The complex energy eigenvalue $-|\epsilon| - i|\Gamma|/2$ of an η-nucleus quasibound state in this work was calculated by solving the momentum space three-dimensional integral equation

$$\frac{\vec{k}'^2}{2\mu}\,\psi(\vec{k}') + \int \mathrm{d}\vec{k}\,\langle \vec{k}'\,|V|\,\vec{k}\,\rangle\psi(\vec{k}) = E\psi(\vec{k}')\,, \tag{2}$$

where $\langle \vec{k}'\,|V|\,\vec{k}\,\rangle$ are momentum space matrix elements of the η-nucleus optical potential V with $\vec{k}$ and $\vec{k}'$ denoting the initial and final η-nucleus relative momenta, respectively. For generating bound states, the ηN values $(0.226{+}i0.094)$ fm and $(0.250{+}i0.123)$ fm were used, which produced η-^{25}Mg states with $E - i\frac{\Gamma}{2} = -(6.5 + i7.1)$ MeV and $-(8.0 + i9.6)$ MeV, respectively. These states along with the non-bound contribution reproduce the experimental peak structure.

2.3 *Conclusion*

With respect to the η-mesic nuclear (quasi)bound states, there definitely exists evidence for their existence in one light and one heavy nucleus, and they are supported by the theoretical efforts. However, this evidence is limited. They need to be (i) confirmed by some other independent experiments and (ii) the quasibound states need to be found in some other nuclei. Such experiments are planned for future study at COSY accelerator and at JPARC.

For completeness we may also state, amongst the unsolved issues in η-nucleus physics, the need to identify appropriate η-production mechanism at energies away from the threshold. The successful two-step model at low energies totally fails to account for the observed characteristics at higher energies [11].

3. K^- bound states

There exists a strangeness -1 resonance, $\Lambda(1405)$, about 28 MeV below the K^-p threshold, width (Γ) $\sim$50 MeV (figure 1). It decays mainly to $\Sigma\pi$ channel. In particle data table this resonance is identified as the bound state of the K^-p system. The line shape of $\Lambda(1405)$ is measured through its $\Sigma^0\pi^0$ decay product in reactions like $pp \to pK^+\Lambda(1405) \to pK^+\Sigma^0\pi^0$, and is found to fit well a single Lorentzian [16]. The K^-p interaction from χPT theories is found to be strongly attractive in s-wave in $T = 0$ state [17,18]. Thus, there is a strong possibility that, in nuclear medium the K^--meson may form bound states, though with large width. Search for such states have been made experimentally, as well as theoretically.

3.1 *Experimental*

First indication of the existence of the K^- bound nuclear states came in 2005 in the FINUDA measurements [19] of the stopped K^- absorption in Li, C and other target nuclei. These experiments using the FINUDA spectrometer installed at the DAΦNE collider detected a Λ hyperon and a proton in coincidence following K^- absorption at rest

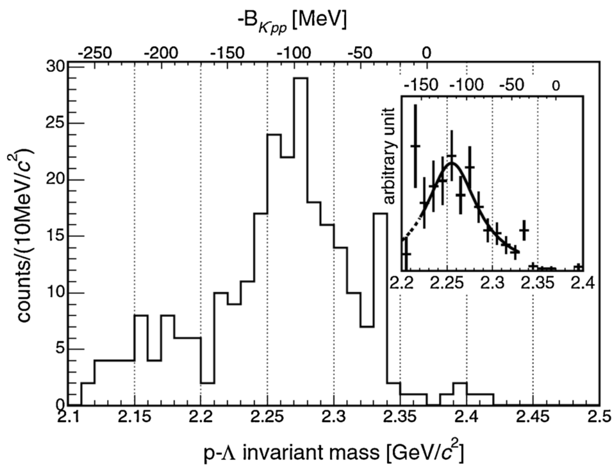

Figure 5. Invariant mass of a Λ and a proton in back-to-back correlation ($\cos\theta_{\text{Lab}} < -0.8$) from light targets before the acceptance correction. The inset shows the result after the acceptance correction for the events which have two protons with well-defined tracks. Only the bins between 2.22 and 2.33 GeV/c^2 are used for the fitting. The plot is taken from [2].

in several nuclei. The emitted $\Lambda - p$ pair was found to emerge, predominantly back to back, in all target nuclei, and had their invariant mass distributions peaking significantly below the sum of a kaon and two proton mass in free state (2.370 GeV) (figure 5). If it is assumed that the Λ–p pair is emitted from a '$K^- pp$' system in the nucleus, this mass shift implies a bound $K^- pp$ system in nuclei with the binding energy above 100 MeV. In a more elaborate second run of these experiments carried out later [20], it was further reported that these mass shifts occur only for the $K^- pp$ module, and not for the $K^- np$ cluster. The absorption on an np pair gives Λ–n and Σ^-–p pairs in the final state.

Recent analysis of the old DISTO data from the Saturne accelerator on $pp \rightarrow p\Lambda K^+$ reaction too suggests the existence of a $K^- pp$ cluster with the binding energy around 100 MeV [21].

As the $K^- N$ interaction in s-state is strongly attractive, the attractive behaviour of the K^--nucleus interaction was expected but the existence of such deeply bound modules came as a big surprise. The occurrence of only '$K^- pp$' modules is understandable because the $K^- N$ interaction is such that it is much stronger in $T = 0$ state than in $T = 1$ state. As the $K^- p$ system is an admixture of $T = 0$ and $T = 1$ states, while the $K^- n$ system is a pure $T = 1$ state, strong interaction between a K^- and a proton is understandable. In the presence of another proton, *a la* Heitler–London theory of hydrogen molecules, K^-, by continuously shuttling between two protons, can understandably cause strong attraction between them, thereby producing bound '$K^- pp$' modules.

3.2 *Theoretical*

Theoretical calculations have been done mainly for the $K^- NN$ system. After identifying a particular framework for calculations, the variational approach [22–27] or the Faddeev

Table 1. Experimental measurements of the $K^- pp$ binding energies and half-widths FINUDA [19] and DISTO [21], $E_B - i\Gamma/2$ (MeV).

FINUDA	DISTO
$115(7) - i67(14)/2$	$103(8) - i118(18)/2$

method [28], all the calculations need to make a realistic choice for the suitable NN and the K^--N potentials. For the NN potential, following extensive work over the years on the subject, it is always possible to make a correct choice. The choice of the $K^- p$ potential, however, is not so certain. In all the calculations, it is chosen such that it gives the 'correct' $\Lambda(1405)$ binding energy. The value of this 'correct' binding energy (BE) depends upon the structure of the 'observed' $\Lambda(1405)$. If it is described as a single pole in the $K^- p$ dynamics, its BE is taken as ∼28 MeV. On the other hand, if it is considered to have, additionally, an admixture of a $\Sigma\pi$ resonance, its BE seems to be smaller (∼12 MeV) (table 1).

Table 2 gives a list of calculated $K^- pp$ binding energies using molecular techniques, Faddeev's method, variational and variational Monte Carlo (VMC) method.

Some of these calculations [2,22,25] also show that the $K^- pp$ module formed in the nuclei is very compact. As an example, table 3 gives results from the single-pole VMC calculations [2].

As we see, the separation of K^- with respect to NN is very small. The NN nucleon core also shrinks considerably. In the $K^- np$ system, e.g., np system shrinks by about 50% compared to deuteron ($\langle R_d^{\rm rms} \rangle = 3.8$ fm). The calculations include the Coulomb interaction.

Comparison of the experimental data (table 1) with the calculated results (table 3) seems to create an impression that the weak $K^- p$ potential from the two-pole chiral perturbation theory is refuted by the experiments. This is likely but not necessarily true. The reasons are three-fold.

(1) The experiments need to be confirmed by other independent experiments.
(2) The structure of the $p\Lambda$ production vertex in the nucleus needs to be understood.
(3) Inclusion of the final-state interaction between the recoiling nucleus and the emerging proton and lambda can be important. This may severely deform the invariant mass spectrum.

While more experiments are planned at JPARC, efforts for reason 2 are not yet forthcoming. Importance of reason 3 is well recognized and findings are reported in [31] and [32].

Table 2. Calculated $K^- pp$ binding energies and half-widths, $E_B - i\Gamma/2$ (MeV).

	Non-χPT				Single pole χPT	Two pole χPT		
	[22,23]	[26]	[28]	[29]	[2,25]	[2]	[24]	[30]
E_B	48	70	55–70	80	124	35–40	20	30–40
Γ	61	85	95–110	73	–	–	20–40	∼50

Table 3. The calculated results for $K^- pp$ and $K^- pn$ systems using Urbana V14 N–N potential for $\langle R_{NN}^{\text{rms}} \rangle$ of NN pair and root mean square radius $\langle R_{(NN)}^{K} \rangle$ of K^- from c.m. of NN pair. All results are in fm.

	$K^- pp$	$K^- np$
NN separation, $\langle R_{NN}^{\text{rms}} \rangle$	1.53	1.85
K^-–NN separation, $\langle R_{(NN)}^{K} \rangle$	0.89	1.24

3.2.1 *Final-state interaction.* The interpretation of the experimentally measured invariant mass distribution [19,21] assumes that the proton and the lambda originating from the production vertex in the nucleus do not undergo any further nuclear interaction. This does not seem to be correct, because, at the energy of outgoing proton and lambda, which being ∼160 MeV, the single nucleon knock-out channel forms the dominant component (∼ 80%) of the reactive proton–nucleus cross-section. Due to this, the outgoing proton and lambda ought to suffer hard scatterings with the nucleon in the nucleus. This will significantly alter their momenta. Consequence of this would be a significant distortion in the invariant mass spectrum of $p\Lambda$.

Two calculations for this study have been done in [31,32]. Both the calculations seem to reproduce the observed mass distribution without invoking any strongly bound $K^- pp$ modules in the nuclei. Calculations in [31] are the computer simulations of the inter-nuclear cascade model for the nucleon–nucleus scattering. This approach describes the sequence of nucleon–nucleon collisions of the outgoing nucleon while passing through

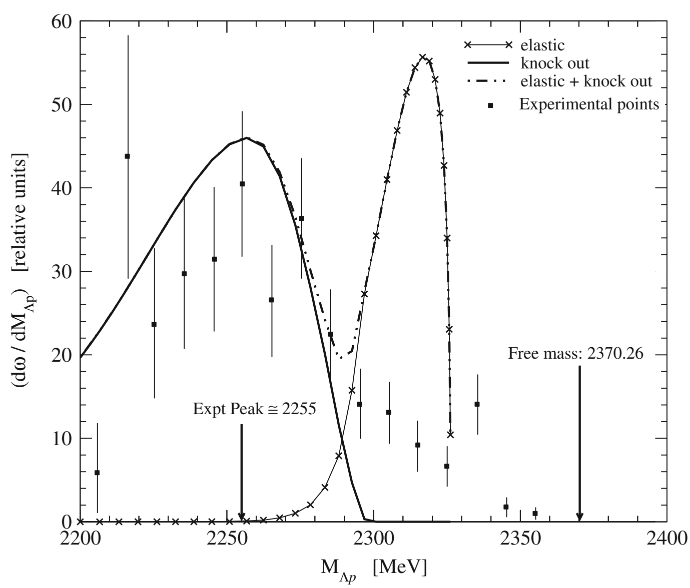

Figure 6. Invariant $p\Lambda$ mass distribution from single nucleon knockout scattering and the elastic scattering in final state [32] along with the experimental points [19].

the residual nucleus in the final state in the framework of classical physics. The trajectory of each nucleon is followed. After a mean free path an N–N collision takes place and its results are computed by Monte Carlo or other similar methods. Apart from the Pauli principle there are no quantum mechanical effects in this approach of describing the FSI. The nucleus too is described by the Fermi gas model, thus being totally devoid of any nuclear structure effect. In view of the crucial role played by the FSI in interpreting the FINUDA Λ-p measurements for K^--nuclear bound states, it is absolutely necessary that the FSI in this reaction is described using quantum mechanical scattering theory and proper nuclear wave functions. Such a calculation was done by Pandejee *et al* [32]. These calculations, while confirming the mass shift due to single nucleon knockout channel, also predict another peak in the $p\Lambda$ invariant mass distribution due to elastic channel in the FSI. The latter peak is not seen in the FINUDA measurements. In figure 6 the calculated $p\Lambda$ invariant mass distribution from [32] is shown.

3.3 *Conclusion*

(1) More experiments are required to confirm the formation of strongly bound K^--nucleus states. Such experiments are planned at JPARC.
(2) If the single nucleon knockout is a genuine candidate for the observed mass shift in FINUDA measurements, experiments must confirm the existence of another peak in the mass measurements corresponding to the elastic scattering in the FSI.
(3) The issue of the structure of the observed $\Lambda(1405)$ resonance needs to be settled.
(4) Study needs to be initiated on the structure of the K^--induced $p\Lambda$ production vertex.

References

[1] N G Kelkar, K G Khemchandani, N J Upadhyay and B K Jain, *Rep. Prog. Phys.* **76**, 066301 (2013)
[2] B K Jain, N J Upadhyay and M Shoeb, *J. Phys. Conf. Ser.* **374**, 012001 (2012)
[3] M Pfeiffer *et al*, *Phys. Rev. Lett.* **92**, 252001 (2004)
[4] A Budzanowski *et al*, *Phys. Rev. C* **79**, 012201 (2009)
[5] M G Betigeri *et al*, *Nucl. Instrum. Methods Phys. Res. Sect. A* **578**, 198 (2007)
[6] Q Haider and L C Liu, *J. Phys. G* **37**, 125104 (2010)
[7] M Ulicny *et al*, *AIP Conf. Proc.* **603**, 543 (2001)
A Budzanowski *et al*, *Phys. Rev. C* **82**, 041001 (2010)
[8] N J Upadhyay, N G Kelkar and B K Jain, *Nucl. Phys. A* **824**, 70 (2009)
[9] P Moskal and J Symrski, *Acta Phys. Polon. B* **41**, 2281 (2010)
[10] N G Kelkar, M Nowakowski, K P Khemchandani and S R Jain, *Nucl. Phys. A* **730**, 121 (2004)
[11] K P Khemchandani, N G Kelkar and B K Jain, *Phys. Rev. C* **68**, 064610 (2003)
K P Khemchandani, N G Kelkar and B K Jain, *Phys. Rev. C* **76**, 0649801 (2007)
K P Khemchandani, N G Kelkar and B K Jain, *Nucl. Phys. A* **708**, 312 (2002)
[12] B Mayer *et al*, *Phys. Rev. C* **53**, 2068 (1996)
[13] E P Wigner, *Phys. Rev.* **98**, 145 (1955)
[14] N G Kelkar, *Phys. Rev. Lett.* **99**, 210403 (2007)
[15] N G Kelkar, K P Khemchandani and B K Jain, *J. Phys. G* **32**, 1157 (2006)
N G Kelkar, K P Khemchandani and B K Jain, *J. Phys. G* **32**, L19 (2006)
[16] I Zychor *et al*, *Phys. Lett. B* **660**, 167 (2008)
[17] N Kaiser, P B Siegel and W Weise, *Nucl. Phys. A* **594**, 325 (1995)

[18] E Oset and A Ramos, *Nucl. Phys. A* **635**, 99 (1998)
J A Oller and U G Meißner, *Phys. Lett. B* **500**, 263 (2001)
M F M Lutz and E E Kolomeitsev, *Nucl. Phys. A* **700**, 193 (2002)
[19] M Agnello *et al*, *Phys. Rev. Lett.* **94**, 212303 (2005)
[20] H Fujioka *et al*, *Nucl. Phys. A* **827**, 303c (2009)
[21] T Yamazaki *et al*, *Proceedings of the International Conference on Exotic Atoms and Related Topics and International Conference on Low Energy Antiproton Physics* (EXA/LEAP 2008) (Vienna, Austria, 2008), arXiv:0810.5182v1
T Yamazaki *et al*, *Phys. Rev. Lett.* **104**, 132502 (2010)
[22] Y Akaishi and T Yamazaki, *Phys. Rev. C* **65**, 044005 (2002)
[23] A Doté, H Horiuchi, Y Akaishi and T Yamazaki, *Phys. Rev. C* **70**, 044313 (2004)
[24] A Doté, T Hyodo and W Weise, *Nucl. Phys. A* **804**, 197 (2008); *Phys. Rev. C* **79**, 014003 (2009)
[25] Mohammad Shoeb and B K Jain, *DAE Symposium on Nuclear Physics* (Roorkee, India, 2008) Vol. 53, p. 561
[26] S Wycech and A M Green, *Phys. Rev. C* **79**, 014001 (2009)
[27] T Hyodo and W Weise, *Phys. Rev. C* **77**, 035204 (2008)
[28] N V Shevchenko, A Gal and J Mares, *Phys. Rev. Lett.* **98**, 082301 (2007)
J Revai, *Phys. Rev. C* **76**, 044004 (2007)
[29] Y Ikeda and T Sato, *Phys. Rev. C* **76**, 035203 (2007)
[30] M Bayer, J Yamagate-Sekihara and E Oset, *Phys. Rev. C* **84**, 015209 (2011)
[31] V K Magas, E Oset, A Ramos and H Toki, *Phys. Rev. C* **74**, 025206 (2006)
[32] G M Pandejee, N J Upadhyay and B K Jain, *Phys. Rev. C* **82**, 034608 (2010)